Flexible Poled and Non-poled PVDF-based Plasmonic THz Sensor for the Detection of Dry Level in Hydrogel Lens

Rahul Karyappa[1], Zhu Qiang [1,2,3*], Xizu Wang[1*] and Karen Ke Lin[1*]

1 . Institute of Materials Research and Engineering (IMRE), Agency for Science, Technology and Research (A*STAR), #08-03, 2 Fusionopolis Way, Innovis, 138634, Singapore.

2 . Institution of Sustainability for Chemical, Energy and Environment (ISCE2), 1 Pesek Road, Jurong Island, Singapore, 627833

3 . School of Chemistry, Chemical Engineering and Biotechnology, Nanyang Technological University, 21 Nanyang Link, Singapore 637371, Republic of Singapore

**Co–first author

* Corresponding author: karen-kl@imre.a-star.edu.sg, wangxz@imre.a-star.edu.sg ,

Abstract: As the most commonly used hydrogel material in contact lenses, the amount of water in a lens affects its optical properties and comfort for the wearer. Therefore, an important challenge is to determine the safety and efficacy of contact lenses by accurately and non-destructively measuring the water content in real time. In this study, we demonstrate the accurate detection of water content in hydrogel contact lenses using a high-precision ATR format in a portable terahertz time-domain spectroscopy system. The technique can resolve small variations in the dielectric constant in solution, which is difficult to achieve with traditional transmission and reflection measurement modes. Information is obtained from the interaction between the sample and the swift waves propagating along the prism surface. The swift waves can excite longitudinal modes that are not directly accessible by conventional techniques. It is worth noting that the reference wave can be measured by removing the sample without disturbing the optical path. We also enhance the plasma effect at the interface with the hydrogel by using PVDF dielectric films of different polarities. We observed that the water content and refractive index changes in the ATR mode show different response patterns for nonpoled PVDF and poled PVDF membranes. This suggests that reflection and relative phase can be accurately evaluated in the THz-ATR technique, resulting in an accurate method for determining complex dielectric constants in the reflection geometry. This will allow accurate measurement of both surface and in vivo water content in hydrogels in the future and is a potential technical route for application in bioaqueous tissue measurements.

KEYWORDS: THz spectra; Contact lens; poled PVDF; water concentration; hydrogel

1. Introduction

A hydrogel, a three-dimensional network of crosslinked hydrophilic polymers, swells in water and maintains structure by holding a large amount of water (about 24 – 78 v/v%)[1-5]. Hydrogels are more suitable to fabricate contact lens as they are soft, optically transparent, biocompatible (required to maintain the corneal and general eyeball physiological conditions) and highly permeable to oxygen[6, 7]. Additionally, hydrogel contact lens improves wearing comfort to the consumers. Over the last five decades, the hydrogel has emerged successful as the material of soft contact lens and others in the commercial market[8-12].

In order to achieve various properties, various functional polymers and hydrogel were deigned and synthesized for biocompatible.[13-17] The key properties of the hydrogels are governed by their water content, mainly the interactions between the polymer and the water, as observed in various aqueous systems.[18-20] The usability of the soft contact lens depends strongly on the free (water that do not interact with the polymer) and bound (water interacting with the polymer) water content, their ability for transport of water

Preprints (www.preprints.org) | NOT PEER-REVIEWED | Posted: 4 May 2023 doi:10.20944/preprints202305.0200.v1

and permeability to oxygen[21-24]. The dehydration of the hydrogel lens is caused by repeated wearing; blinking of the eyes cause air drying (open eye) and rehydration (closed eye)[25]. Moreover, it is influenced by several factors such as ambient conditions[26, 27], thickness[21], and the use of surfactant[28]. Dehydration of hydrogel lens can induce complications associated with discomfort due to – (1) mismatch between the lens and the outer shape of the eyeball, and (2) diminishing adhesive forces between the lens and the cornea[29-31]. Additionally, it can modify important properties such as radius of curvature, permeability to oxygen, and wettability[32-35]. Since dehydration is critical in the functionality of the hydrogel contact lens, it is inevitable – (1) to develop new polymers for the fabrication of the contact lens, (2) to optimize of different types of existing contact lenses, and (3) to develop methods to determine the water content of the contact lens.

Several methods have been demonstrated for measuring water content of the hydrogel contact lenses. Traditionally two methods have been used. The first method was based on the refractive index, although simple in use, it was inaccurate[23, 36-39]. Another method was developed based on a gravimetric technique[39-43]. The water content in the contact lens was accurately measured before and after drying. The overestimation of the true water content is possible if the moisture on the surface is not removed prior to weighing. The other methods to determine the water content in the contact lens included sorption/desorption experiments[44], nuclear magnetic resonance (NMR)[45, 46], Raman spectroscopy[47], and Fourier transform infrared (FTIR) spectroscopy[48, 49]. An aquaphotomics approach based on near-infrared (NIR) spectroscopy and multivariate analysis was developed[50]. It is a rapid and non-invasive method to examine the state of water in the hydrogel contact lens. Recently a novel tetrahertz (THz = 10^{12} Hz) system was demonstrated to study the dehydration process of different hydrogel contact lenses[51]. THz radiation possess unique properties, non-invasive technique with non-ionizing properties, that are suitable for biomedical research[52]. The energy of THz corresponds to the intermolecular oscillations that can identify orientations of crystal of the same molecule. THz radiation is used to determine water content of living cells and biomaterials[53], leaves[54], drying paint[55], and imaging for diagnosis of cancer[56].

Terahertz (THz) molecular spectroscopy provides considerable scientific potential as numerous absorption, and emission lines of molecules of interest in the chemical sciences belong to this spectral region, where various chemical species exhibit strong characteristic rotational and rovibrational transitions. Electromagnetic waves with frequencies between 0.3 – 10 THz or millimetre-wavelength (3 – 300 cm−1) are defined as THz radiation. They are included in the electromagnetic spectrum between the microwave or millimetre and the far-infrared regions. The energy for molecular rotations in the gas phase, crystalline phonon vibrations, low-frequency vibrations, and intermolecular vibrations in the solid-state fall in the THz energy range. In this THz energy range, numerous biological and chemical compounds exhibit characteristic absorptions and dispersions because of vibrational transitions, mostly collective and intermolecular vibrational modes. These THz vibrational modes provide fingerprint information for the identification of organic molecules. Therefore, THz molecular spectroscopy has been widely used in chemistry and related fields[57].

In this work, we used the THz time-domain spectroscopy, which includes the usage of attenuated total reflection (ATR) spectroscopy mode for enhanced signal SNR measurement. By incorporating high precision ATR mode in a portable terahertz time-domain spectroscopy system, we demonstrated accurate detection of moisture levels in the hydrogel contact lens. THz time-domain ATR spectroscopy enabled us an accurate measurement of the complex dielectric function of the analyte, either in liquid or gaseous states. This technique made it possible to resolve slight changes in dielectric constants in solution, a goal that is difficult to achieve with the conventional transmission and reflection measurement mode. ATR mode provides information on the interaction between the sample and the evanescent wave traveling along a prism surface. The evanescent wave can excite longitudinal modes that are not accessed directly by conventional techniques. It is noteworthy that the reference wave can be measured by removing the sample without arranging the optical pathways. It shows that the reflection and relative phases can be evaluated

 doi:10.20944/preprints202305.0200.v1

accurately in the THz-ATR technique, resulting in an accurate method to determine complex dielectric constants in reflection geometry. As a result, the proposed method is successful in improving the calculation of the optical properties of the samples.

2. Experimental Section

We employed 2 contact methodologies and 2 types PVDF film attenuated total reflection (ATR) mode. Figure 1(a) shows the lab setting picture of THz-TDS in transmission mode and method, Figure 1(b) shows the schematic diagram of THz-TDS in Attenuated Total Reflection (ATR) setup. We used TERA K15 (Menlo Systems GmbH, Germany) as source system in our experiments. The two femtosecond fibre lasers with 250 MHz repetition rate and 90 femtosecond laser pulses with around 1.56 μm central wavelength are used to excite two photoconductive antennas namely emitter and receiver with the coverage of bandwidth up to 3.5 THz. The THz beam is focused with TPX lenses, and the size of the focus beam is approximately 1 mm with maximum THz output of 0.3 THz. The THz focused beam was shone on the leaf surface and transmitted beam was collected. The ATR prism, made of silicon crystal was placed at the focal position of the THz radiation. The incident angle of the THz pulse on the prism surface was 57-degree. The complex dielectric constant was measured from 0.15 to 4.0 THz, with the frequency resolution set at 7.6 GHz. For the ATR test, the reference spectrum is obtained by scanning air (sample holder without sample) with an integration time of 20 seconds too.

For ATR test, the 2 types PVDF was developed to enhance the surface plasmonic with contact lens during the measurement. A polyvinylidene fluoride (PVDF) polymer with molecular weight (MW) of ~534,000 (Sigma Aldrich), N, N-dimethylformamide (DMF) (Merck), acetone (Merck), and commercial sugar ($C_{12}H_{22}O_{11}$) was used in this work. Dissolving the PVDF polymer powder in a DMF/acetone mixture produced the PVDF solutions (50:50 in volume). 12 hours at 60 °C in a silicone oil bath with stirring was required to completely dissolve the polymer. The PVDF foam (F-PVDF) was fabricated by mixing the PVDF solution with commercially available sugar to form a dough-like mixture with a polymer-to-sugar mass ratio of 1:9. As soon as the mixture had been formed, it was immediately dried in an oven at 100 °C to remove excess solvents and ensure complete drying of the mixture. To obtain a porous structure, the sample was removed from the mold and leached (rinsed) repeatedly in hot water to remove the sugar. On the other hand, the samples were dried in an oven for 12 hours at 100 °C. A sample pellet with a thickness of ~ 0.273 mm and ~ 1.5 cm was made with hydraulic pressure using ~ 46 MPa at room temperature. The corona poling method was used to stimulate the formation of poled PVDF film (polar β-phase in F-PVDF), which involves raising the needle to a high potential enough to cause a partial breakdown of the air around the needle. The surrounding air is then ionized. These ions fall down towards the sample, causing a charge build-up on the surface and raising the surface potential. Poling was carried out on a small circular disk of F-PVDF, cut into 270 μm thickness and charged at 60 kV. The distance between the sample's surface and the needle was set at 3 mm. To ensure the flatness of the interface during ATR testing, all PVDF films are covered with a 0.5 mm thick silicon wafer.

Preprints (www.preprints.org) | NOT PEER-REVIEWED | Posted: 4 May 2023 doi:10.20944/preprints202305.0200.v1

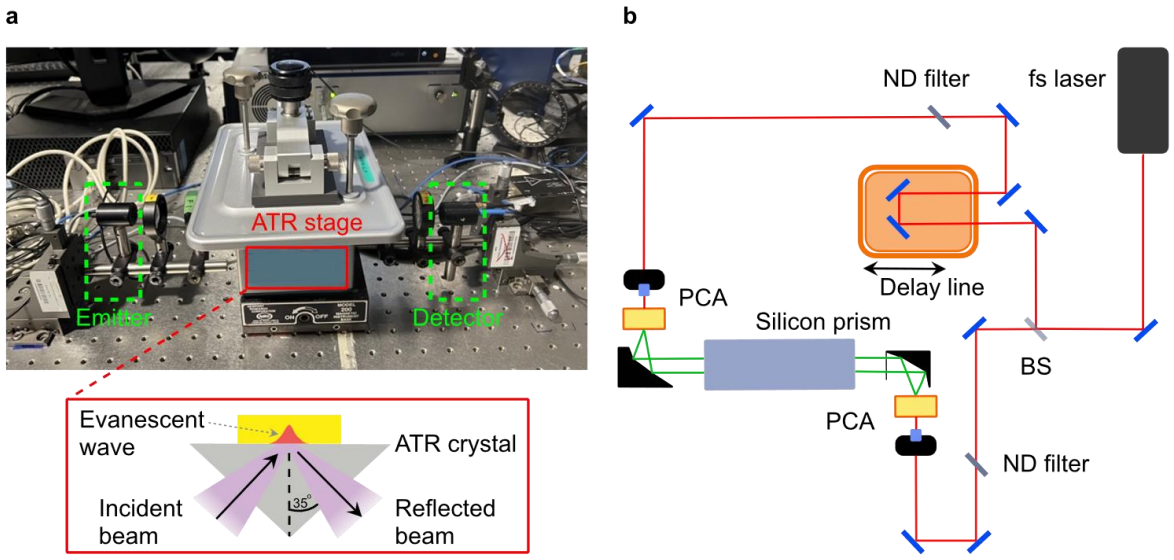

Figure 1. An Image (a) and a schematic diagram of ATR method on PVDF-based plasmonic THz sensor for the detection of water in the hydrogel lens.

The 270 μm thick PVDF film was deposited on a 1 mm thick high resistivity Si (100) substrate by spin coating. We selected two setups of measurements: (1) Face-down – the hydrogel lens was pressed down by Si/PVDF substrate on the top surface of prism, and (2) Face-up – the hydrogel lens was pressed down on the top of Si/PVDF substrate placed on top of the prism. The enlarged ATR measurement module is shown in Fig. 1(b). A prism was put under the Si substrate to refract the THz light into the sample for first measurement setup, while THz light focus on the Si plate with a desired incident angle to the Si-PVDF interface in the second measurement setup. In both the cases the TIR condition should be met. A fiber-coupled THz-TDS system was established for the measurement. The system was built based on Tera K15 from Menlo Systems GmbH. In the THz experimental system, femtosecond fibre lasers with 250 MHz repetition rate and 90 femtosecond laser pulses with around 1.56 μm central wavelength are used to excite two photoconductive antennas, one is used as emitter and another is used as receiver, which are fibre-coupled. The THz pulse is generated with the coverage of bandwidth up to 3 THz. The incident angle of the ATR setup is XX degree. The THz beam was manipulated by a set of TPX lenses and focused onto the Si-PVDF interface.

Preprints (www.preprints.org) | NOT PEER-REVIEWED | Posted: 4 May 2023 doi:10.20944/preprints202305.0200.v1

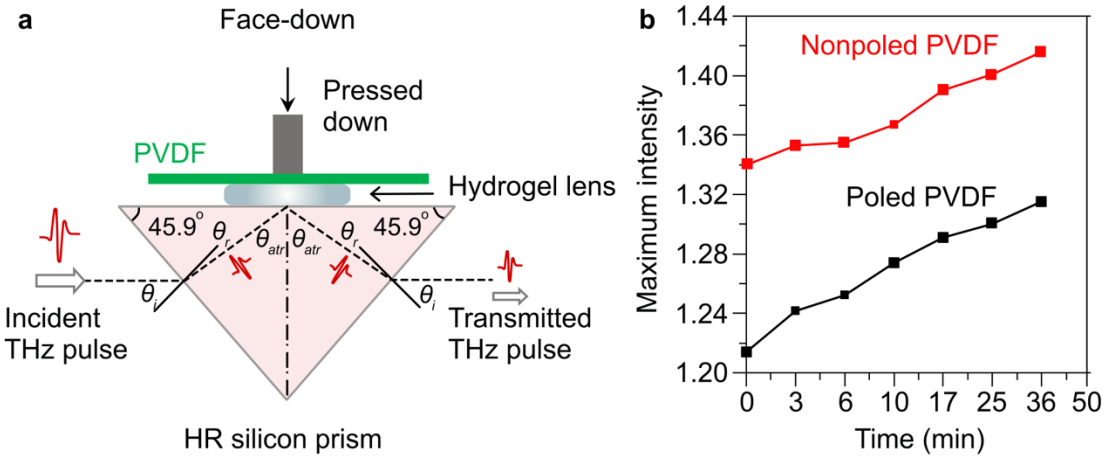

Figure 2. A schematic diagram of a PVDF sensor with a face-down method for the detection of water content in the hydrogel lens (a), and the THz intensity response of the water level on non-poled and poled PVDF sensor (b).

In the face-down method, the lens focal was between the PVDF sensor and Si prism. THz light passed through the whole hydrogel lens due to the strong absorption of THz wavelength in water. The face-down arrangement detected most of the absorption intensity from the hydrogel sample. The hydrogel dried as time progressed, causing a reduction in the absorption intensity and an increase in reflection. The absorption intensity increased with the exposure time of the lens. The non-poled PVDF showed high reflection signal intensity with low sensitivity $\frac{\Delta D}{D_o} < 6.2\%$, while poled PVDF showed high sensitivity, $\frac{\Delta D}{D_o} > 9.0\%$, after 36 min. The piezoelectric coefficient of PVDF reduced the background intensity and detected the high response signal. However, the reflection intensity of the poled PVDF sensor was lower than that of the non-poled PVDF due to the high interface absorption and interaction between poled PVDF and the sample at the PVDF/hydrogel lens interface. The face-down ATR mothed was very sensitive to the amount of water in the hydrogel with the poled PVDF suggesting its strong interfering effects with the sample.

Preprints (www.preprints.org) | NOT PEER-REVIEWED | Posted: 4 May 2023 doi:10.20944/preprints202305.0200.v1

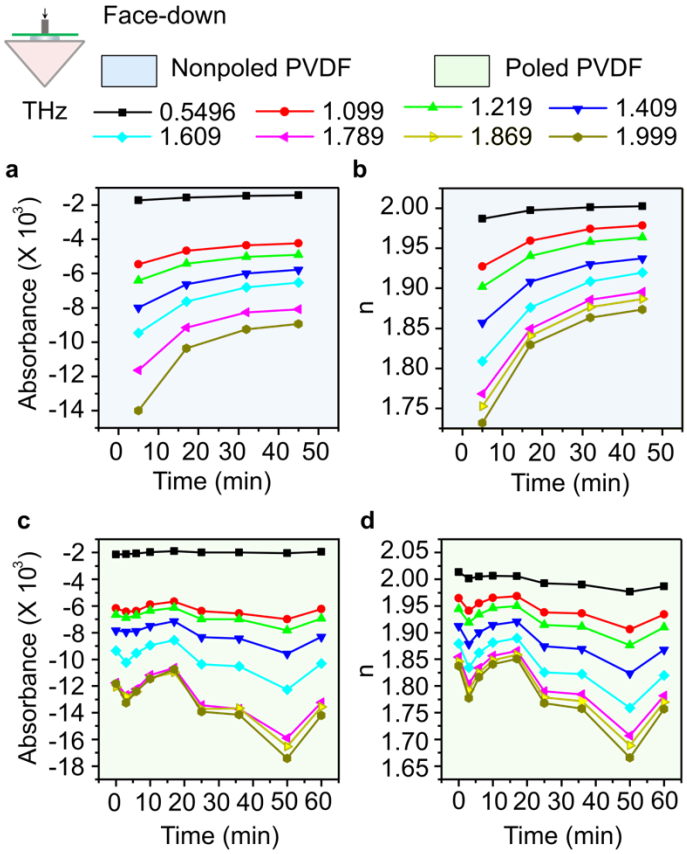

Figure 3. The absorbance (a) and THz refractive index (b) as a function of frequency for face-down method with non-poled PVDF sensor, exposure times from 0 to 60 min. The absorbance (c) and THz refractive index (d) as a function of frequency for face-down method with poled PVDF sensor with an exposure time from 0 to 60 min.

The absorbance and the reflection index (n) at different THz wavelengths with the time of test are plotted for the face-down method (Fig. 3). The poled PVDF exhibited the same attenuation phenomenon as non-poled films during the hydrogel dehydration. However, the polarized films showed more characteristic absorption peaks and a lower absorption background due to strong interface absorption at the poled PVDF/hydrogel lens interface. The water/poled PVDF interface displayed increased spectrum response at THz wavelength, possibly due to the interface plasmonic effect, which is more sensitive at a particular THz wavelength. For poled PVDF, the value of n did increase with the increase in the dryness of the hydrogel at higher frequencies (> 1.5 Hz). The strong interaction at the poled PVDF/hydrogel interface than that of the non-poled PVDF/hydrogel interface reduced the total reflection THz broadband signal. Overall, the face-down method can be used to obtain water content in the hydrogel. The strong reflection intensity of the non-poled PVDF at THz effectively obtained information on the varying water content in the hydrogel during the observation period.

Preprints (www.preprints.org) | NOT PEER-REVIEWED | Posted: 4 May 2023 doi:10.20944/preprints202305.0200.v1

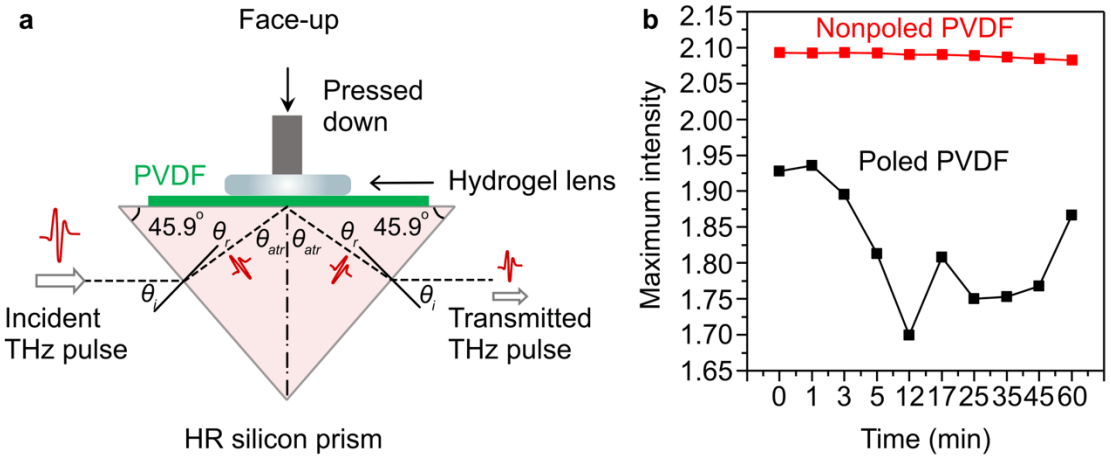

Figure 4. A schematic diagram of a PVDF sensor with a face-up method for the detection of water content in the hydrogel lens (a), and the THz intensity response of the water level on non-poled and poled PVDF sensor (b).

In order to get more information about the interface, we wanted the light to pass through the water/hydrogel interface first. Therefore we used an face-up approach for the measurement. The overall signal in the face-up method was higher than the face-down method for both poled and non-poled PVDF. The high resistivity of Si/PVDF had higher transmission. In the non-poled PVDF film, the decrease in the absorption intensity was lower than the face-down method due to more response signal from the interface. However, the non-poled PVDF/hydrogel interface was not sensitive at THz wavelength. The poled PVDF enhances the surface plasmonic effect due to strong dielectric features [REF]. The more loss in the absorption intensity with the exposed time, highlighted the faster loss of water from the hydrogel surface than in the hydrogel body (Fig. 4b). It is clear that compared to nonpoled PVDF as a result of the probe film poled PVDF derives from enhanced surface plasma effects due to its strong dialectical properties. In Fig. 4b, as the exposure time increases, loses more of its absorption intensity in the first 12 minutes, which means that water is lost from the surface of the hydrogel more quickly than from the body of the hydrogel. Also, the order of the PVDF/contact lens interface shows the intensity of the different interface signals; face down: first the THz wave passes through the hydrogel before reaching the interface with PVDF, with the plasmonic effect as an aid. Face up: first THz waves pass through the plasmonic interface before reaching the upper body of the hydrogel. This assumes that we can observe more loss of water absorption intensity at different locations of the contact lens through the polarisation detector as well as the order of the interfaces.

2. At face-up method of ploed PVDF means that this is a non-destructive and fast way to detect the distribution and changes in water content of contact lenses and other hydrogel-like materials.

Preprints (www.preprints.org) | NOT PEER-REVIEWED | Posted: 4 May 2023 doi:10.20944/preprints202305.0200.v1

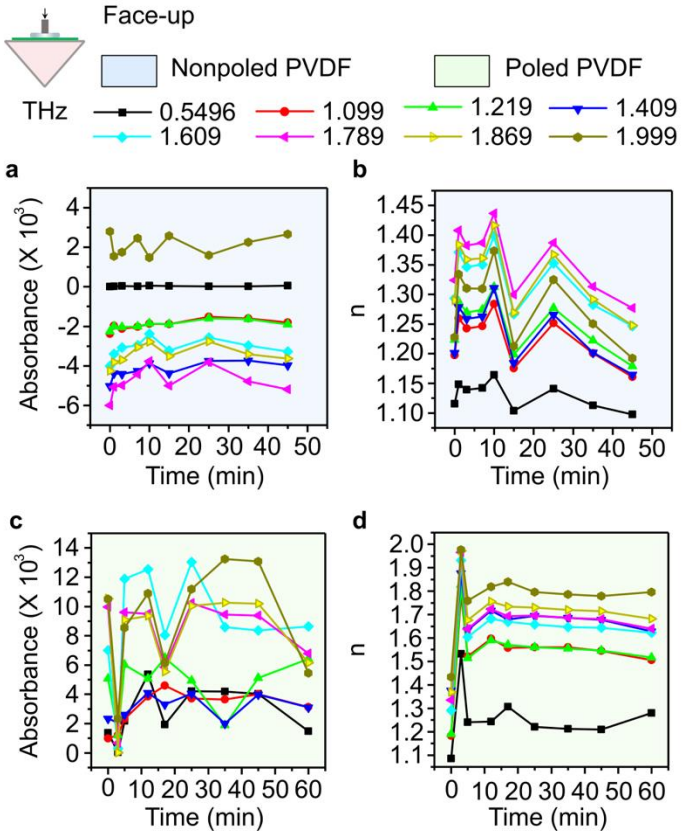

Figure 5. The absorbance (a) and THz refractive index (b) as a function of frequency for face-up method with non-poled PVDF sensor, exposure times from 0 to 60 min. The absorbance (c) and THz refractive index (d) as a function of frequency for face-up method with poled PVDF sensor with an exposure time from 0 to 60 min.

In the face-up method, the attenuation amplitude increased significantly in the plasmonic test model suggesting considerable increase in the sensitivity of the detection $\left(\frac{\Delta D}{D_o} > 30\%\right)$. The plasmonic enhanced the absorption in the poled PVDF sensor and change in reflex index information. The non-poled PVDF provided information only on water loss, although less than the face-down method due to shorter light transmission path than in face-up method. Few absorption peaks were observed, although insignificant, in case of non-poled PVDF face-up method compared to face-down method. However, more peak information was obtained in poled PVDF face-up method compared to face-down method. The plasmonic effect enhanced THz transfer to the contact lens, which induced more information at the interface than the non-poled PVDF sensor (Fig. 5a and 5b). A downward trend was observed in the intensity of the absorption peaks for 0–5 min, which was significantly different from the samples tested in other modes (Fig. 5c-5d). The trend suggested a presence of water at the PVDF/hydrogel interface in the poled PVDF for 0–5 min. As shown in Fig 5c, in the high frequency section (1.6-2.0Hz) the absorption changes are more pronounced, but the noise is also strong. This is likely to be the response of other organic molecular bonds in the contact lens to the spectrum. In contrast, in Figure 5d, it can be seen that the higher frequencies have a higher reflex index n, and all show a consistent enhancement in the first 5 minutes, which then diminishes and stabilises. This also verifies that there is a process of interfacial water composition change and stabilisation at the

Preprints (www.preprints.org) | NOT PEER-REVIEWED | Posted: 4 May 2023 doi:10.20944/preprints202305.0200.v1

interface between the poled PVDF and the contact lens. This signal can only be amplified by the enhancement of the surface plasmonic effect. The interfacial water content reached equilibrium for time greater than 5 min suggesting start of water loss from the contact lenses at the interface, which is not reported in the previous detection methods [REF].

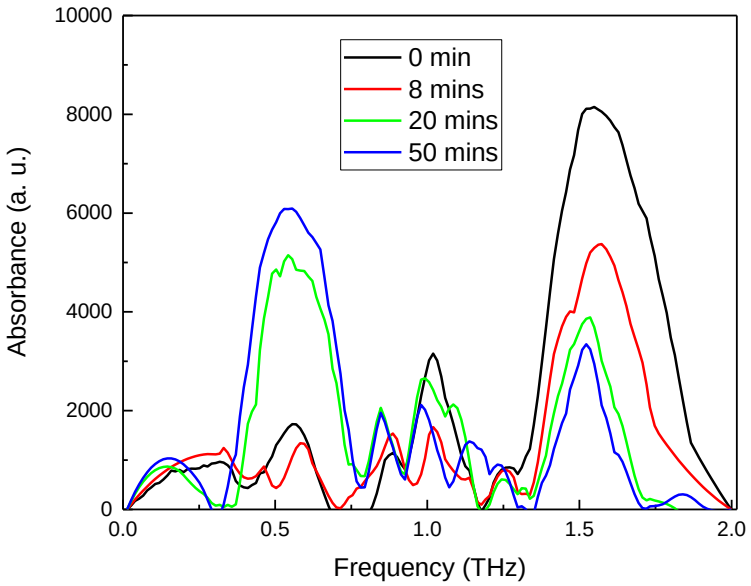

Figure 6. The absorption spectra of the hydrogel lens at the sensor surface at different times, (a) 0min, (b) 8 min, (c) 20 min and (d) 50 min.

Figure 6 gives the variation of the THzp spectrum between 0 and 2Thz with time, with different shifts and changes in the spectrum in each band as expected. The water absorption shows broad peaks at around 1.1 THz and 1.6–2 THz. The front peak below 1 THz was from the polymer chemicals. A peak was observed from 0.4–1.6 THz after 3 min (Fig. 6a). Apparently at the beginning the water absorption frequency peak shows a high intensity and a large amount of water is observed in the sample surface. However, as time progresses the water peak diminishes, and the chemical fingerprint peak becomes more pronounced. This just dynamically indicates that water starts to be gradually lost from the surface of the contact lens. As can be seen, our established test model suggests that poled PVDF in face-up mode is more sensitive to the water content of the hydrogel interface. With detailed calibration of the individual characteristic peaks and j-calibration, the water, organic and chemical content of the hydrogel material can be detected more accurately in the future.

3. Conclusions

By employing high precision ATR modes in a portable terahertz time-domain spectroscopy system and attempting to optimise and analyse information about the interaction between the sample and the swift waves propagating along the prism surfacel to detect changes in the surface and body water content of hydrogels. The testing and optimisation of the plasma effects at the medium/hydrogel interface resulted in an accurate method for determining complex dielectric constants in the reflection geometry based on the THz-ATR technique. This provides a novel detection method for the future accurate measurement of the content and distribution of water components in biological materials.

Author Contributions: Wang Xizu and Rahul Karyappa contributed to writing – original draft and review & editing. Ke Lin and Zhu Q. contributed to investigation and methodology.

Conflicts of interest: There are no conflicts to declare.

Acknowledgements: We would like to acknowledge the A*STAR, SERC Thermoelectric Materials Program (grant numbers: 1527200019, 1527200024 & 1527200021) and Sustainable Hybrid Lighting System for Controlled Environment Agriculture Program (grant numbers: A19D9a0096).

References

1. Loh, X. J.; Guerin, W.; Guillaume, S. M., Sustained delivery of doxorubicin from thermogelling poly (PEG/PPG/PTMC urethane) s for effective eradication of cancer cells. *Journal of Materials Chemistry* **2012,** *22* (39), 21249-21256.

2. Loh, X. J.; Nguyen, V. P. N.; Kuo, N.; Li, J., Encapsulation of basic fibroblast growth factor in thermogelling copolymers preserves its bioactivity. *Journal of materials chemistry* **2011,** *21* (7), 2246-2254.

3. Li, Z.; Chee, P. L.; Owh, C.; Lakshminarayanan, R.; Loh, X. J., Safe and efficient membrane permeabilizing polymers based on PLLA for antibacterial applications. *Rsc Advances* **2016,** *6* (34), 28947-28955.

4. Gan, L.; Deen, G. R.; Loh, X.; Gan, Y., New stimuli-responsive copolymers of N-acryloyl-N′-alkyl piperazine and methyl methacrylate and their hydrogels. *Polymer* **2001,** *42* (1), 65-69.

5. Wang, S.; Ong, P. J.; Liu, S.; Thitsartarn, W.; Tan, M. J. B. H.; Suwardi, A.; Zhu, Q.; Loh, X. J., Recent Advances in Host-Guest Supramolecular Hydrogels for Biomedical Applications. *Chemistry–An Asian Journal* **2022,** *17* (18), e202200608.

6. Metha, A. B.; Crane, A. M.; 3rd, H. G. R.; Thomsen, S. L.; Albrecht, D. G., Maintaining the Cornea and the General Physiological Environment in Visual Neurophysiology Experiments. *J. Neurosci. Methods* **2001,** *109*, 153-166.

7. Childs, A.; Li, H.; Lewittes, D. M.; Dong, B.; Liu, W.; Shu, X.; Sun, C.; Zhang, H. F., Fabricating Customized Hydrogel Contact Lens. *Sci. Rep.* **2016,** *6*, 34905.

8. Carnt, N.; Gonzalez-Garcia, M. J., The R-evolution of Contact Lenses: Will Long-term Contact Lens Wearers in the Future be the Same as Now? *Cont. Lens Anterior Eye* **2022,** *45*, 101557.

9. Loh, X. J., Poly (DMAEMA-co-PPGMA): Dual-responsive "reversible" micelles. *Journal of applied polymer science* **2013,** *127* (2), 992-1000.

10. Nguyen, V. P. N.; Kuo, N.; Loh, X. J., New biocompatible thermogelling copolymers containing ethylene-butylene segments exhibiting very low gelation concentrations. *Soft Matter* **2011,** *7* (5), 2150-2159.

11. Fan, X.; Tan, B. H.; Li, Z.; Loh, X. J., Control of PLA stereoisomers-based polyurethane elastomers as highly efficient shape memory materials. *ACS Sustainable Chemistry & Engineering* **2017,** *5* (1), 1217-1227.

12. Wang, S.; Wu, W. Y.; Yeo, J. C. C.; Soo, X. Y. D.; Thitsartarn, W.; Liu, S.; Tan, B. H.; Suwardi, A.; Li, Z.; Zhu, Q., Responsive hydrogel dressings for intelligent wound management. *BMEMat* **2023**, e12021.

13. Soo, X. Y. D.; Png, Z. M.; Wang, X.; Chua, M. H.; Ong, P. J.; Wang, S.; Li, Z.; Chi, D.; Xu, J.; Loh, X. J., Rapid UV-curable form-stable polyethylene-glycol-based phase change material. *ACS Applied Polymer Materials* **2022,** *4* (4), 2747-2756.

14. Lee, J. J. C.; Sugiarto, S.; Ong, P. J.; Soo, X. Y. D.; Ni, X.; Luo, P.; Hnin, Y. Y. K.; See, J. S. Y.; Wei, F.; Zheng, R., Lignin-g-polycaprolactone as a form-stable phase change material for thermal energy storage application. *Journal of Energy Storage* **2022,** *56*, 106118.

15. Wang, S.; Muiruri, J. K.; Soo, X. Y. D.; Liu, S.; Thitsartarn, W.; Tan, B. H.; Suwardi, A.; Li, Z.; Zhu, Q.; Loh, X. J., Bio-Polypropylene and Polypropylene-based Biocomposites: Solutions for a Sustainable Future. *Chemistry, an Asian Journal* **2022**, e202200972-e202200972.

16. Muiruri, J. K.; Yeo, J. C. C.; Soo, X. Y. D.; Wang, S.; Liu, H.; Kong, J.; Cao, J.; Tan, B. H.; Suwardi, A.; Li, Z., Recent Advances of Sustainable Short-chain length Polyhydroxyalkanoates (Scl-PHAs)–Plant Biomass Composites. *European Polymer Journal* **2023**, 111882.

17. Png, Z. M.; Wang, C.-G.; Yeo, J.; Lee, J. J. C.; Surat'man, N. E. B.; Tan, Y. L.; Liu, H.; Wang, P.; Tan, M. B. H.; Xu, J., Stimuli-responsive Structure-Property Switchable Polymer Materials. *Molecular Systems Design & Engineering* **2023**.

18. Yildirim, E.; Zhu, Q.; Wu, G.; Tan, T. L.; Xu, J.; Yang, S.-W., Self-organization of PEDOT: PSS induced by green and water-soluble organic molecules. *The Journal of Physical Chemistry C* **2019,** *123* (15), 9745-9755.

19. Zhu, Q.; Yildirim, E.; Wang, X.; Kyaw, A. K. K.; Tang, T.; Soo, X. Y. D.; Wong, Z. M.; Wu, G.; Yang, S.-W.; Xu, J., Effect of substituents in sulfoxides on the enhancement of thermoelectric properties of PEDOT: PSS: experimental and modelling evidence. *Molecular Systems Design & Engineering* **2020,** *5* (5), 976-984.

20. Tang, T.; Kyaw, A. K. K.; Zhu, Q.; Xu, J., Water-dispersible conducting polyazulene and its application in thermoelectrics. *Chemical Communications* **2020,** *56* (65), 9388-9391.

21. Andrasko, G., Hydrogel Dehydration in Various Environments. *Int. Contact Lens Clin.* **1983,** *10*, 22-28.

22. Tranoudis, I.; Efron, N., Water Properties of Soft Contact Lens Materials. *Cont. Lens Anterior Eye* **2004,** *27*, 193-208.

23. Brennan, N.; Efron, N.; Bruce, A.; Duldig, D.; Russo, N., Dehydration of Hydrogel Lenses: Environmental Influences During Normal Wear. *Am. J. Optom. Physiol. Opt.* **1988,** *65*, 277-281.

24. Benz, P.; Ors, J., New Materials Demand More Accurate Measurements of Performance. *Spectrum* **1997,** *12*, 40-46.

25. Eftimov, P.; Yokoi, N.; Peev, N.; Georgiev, G. A., Impact of Air Exposure Time on the Water Contact Angles of Daily Disposable Silicone Hydrogels. *Int. J. Mol. Sci.* **2019,** *20*, 1313.

26. Caló, E.; Khutoryanskiy, V. V., Biomedical Applications of Hydrogels: A Review of Patents and Commercial Products. *Eur. Polym. J.* **2015,** *65*, 252-267.

27. Fatt, I.; Chaston, J., The Effect of Temperature on Refractive Index, Water Content and Central Thickness of Hydrogel Contact Lenses. *Int. Contact Lens Clin.* **1980,** *7*, 250-255.

28. Marx, S.; Sickenberger, W., A Novel In-Vitro Method for Assessing Contact Lens Surface Dewetting: Noninvasive Keratograph Dry-up Time (NIK-DUT). *Cont. Lens Anterior Eye* **2017,** *40*, 382-388.

29. Weed, K.; Fonn, D.; Potvin, R., Discontinuation of Contact Lens Wear. *Optom. Vis. Sci.* **1993,** *70*, 140.

30. Zhu, D.; Liu, Y.; Gilbert, J. L., Micromechanical Measurement of Adhesion of Dehydrating Silicone Hydrogel Contact Lenses to Corneal Tissue. *Acta Biomater.* **2021,** *127*, 242-251.

31. Holden, B.; Sweeney, D.; Seger, R., Epithelial Erosions Caused by Thin High Water Content Lenses. *Clin Exp Optom* **1986,** *69*, 103-107.

32. Lin, C.; Cho, H.; Yeh, Y.; Yang, M., Improvement of the Surface Wettability of Silicone Hydrogel Contact Lenses via Layer-by-Layer Self-Assembly Technique. *Colloids Surf. B Biointerfaces* **2015,** *136*, 735-743.

33. Tranoudis, I.; Efron, N., In-eye Performance of Soft Contact Lenses Made from Different Materials. *Cont. Lens Anterior Eye* **2004,** *27*, 133-148.

34. Rajchel, D.; Krysztofiak, K.; Szyczewski, A., Influence of Sodium Hyaluronate on Dehydration and Water Distribution in Soft Contact Lenses. *Opt. Appl.* **2016,** *46*, 483-496.

35. Efron, N.; Morgan, P. B., Hydrogel Contact Lens Dehydration and Oxygen Transmissibility. *Clao. J.* **1999,** *25*, 148-151.

36. Efron, N.; Brennan, N.; Bruce, A.; Duldig, D.; Russo, N., Dehydration of Hydrogel Lenses under Normal Wearing Conditions. *CLAO J.* **1987,** *13*, 152-156.

37. Mousa, G.; Callender, M.; Sivak, J.; Egan, D., The Effect of the Hydration Characteristics of Hydrogel Lenses on the Refractive Index. *Int. Contact Lens Clin.* **1983,** *10*, 31-37.

38. Brennan, N., A Simple Instrument for Measuring the Water Content of Hydrogel Lenses. *Int. Contact Lens Clin.* **1983,** *10*, 357-362.

39. Galas, S.; Enns, J., Humidity-conditioned Gravimetric Method to Measure the Water Content of Hydrogel Contact Lens Materials. *Optom. Vis. Sci.* **1993,** *70*, 577-586.

40. Helton D, W. L., Hydrogel Contact Lens Dehydration Rates Determined by Thermogravimetric Analysis. *CLAO J.* **1991,** *17*, 59-61.

41. Mirejovsky, D.; Patel, A.; Young, G., Water Properties of Hydrogel Contact Lens Materials: A Possible Predictive Model for Corneal Desiccation Staining. *Biomaterials* **1993,** *14*, 1080-1088.

42. McConville, P.; Pope, J. M., Diffusion Limited Evaporation Rates in Hydrogel Contact Lenses. *CLAO J.* **2001,** *27*, 186-191.

43. Jones, L.; May, C.; Nazar, L.; Simpson, T., In Vitro Evaluation of the Dehydration Characteristics of Silicone Hydrogel and Conventional Hydrogel Contact Lens Materials. *Cont. Lens Anterior Eye* **2002,** *25*, 147-156.

44. Sun, Y.-M.; Lee, H.-L., Sorption/desorption properties of water vapour in poly(2-hydroxyethyl methacrylate): 1. Experimental and preliminary analysis. *Polymer* **1996,** *37*, 3815-3818.

45. Larsen, D. W.; Huff, J. W.; Holden, B. A., Proton NMR Relaxation in Hydrogel Contact Lenses: Correlation with In Vivo Lens Dehydration Data. *Curr. Eye Res.* **1990,** *9*, 697-706.

46. McConville, P.; Pope, J. M., 1H NMR T_2 Relaxation in Contact Lens Hydrogels as a Probe of Water Mobility. *Polymer* **2001,** *42*, 3559-3568.

47. Sekine, Y.; Ikeda-Fukazawa, T., Structural Changes of Water in a Hydrogel During Dehydration. *J. Chem. Phys.* **2009,** *130*, 034501.

48. Yin, L.; Zhao, Z.; Hu, Y.; Ding, J.; Cui, F.; Tang, C.; Yin, C., Polymer-Protein Interaction, Water Retention, and Biocompatibility of a Stimuli-sensitive Superporous Hydrogel Containing Interpenetrating Polymer Networks. *J. Appl. Poly. Sci.* **2008,** *108*, 1238-1248.

49. Anbudayanidhi, S.; Nayak, S. K.; Mohanty, S., Synthesis and Water State Characterization of Polysodium Acrylate/Cellulose Microfibril Hydrogels. *J. Thermoplast. Compos. Mater.* **2014,** *27*, 573-585.

50. Munćan, J.; Mileusnić, I.; Rosić, J. Š.; Vasić-Milovanović, A.; Matija, L., Water Properties of Soft Contact Lenses: A Comparative Near-Infrared Study of Two Hydrogel Materials. *Int. J. Polym. Sci.* **2016,** *2016*, 3737916.

51. Burgos-Fernández, F. J.; Guaus, E.; Martínez, C.; Vilaseca, M., Terahertz-based System for Dehydration Analysis of Hydrogel Contact Lenses. *Opt. Appl.* **2019,** *49*, 571-584.

52. Yang, X.; Zhao, X.; Yang, K.; Liu, Y.; Liu, Y.; Fu, W.; Luo, Y., Biomedical Applications of Terahertz Spectroscopy and Imaging. *Trends Biotechnol.* **2016,** *34*, 810-824.

53. Shirga, K.; Suzuki, T.; Kondo, N.; Tanaka, K.; Ogawa, Y., Hydration State Inside HeLa Cell Monolayer Investigated with Terahertz Spectroscopy. *Appl. Phys. Lett.* **2015,** *106*, 253701.

54. Gente, R.; Koch, M., Monitoring Leaf Water Content with THz and sub-THz Waves. *Plant Methods* **2015,** *11*, 15.

55. Shen, Y.-C., Terahertz Sensor for Noncontact and Non-destructive Inspection of Automotive Paints. *Int. J. Sens. Netw. Data Commun.* **2014,** *4*, e103.

56. Rahman, A.; Rahman, A. K.; Rao, B., Early Detection of Skin Cancer via Terahertz Spectral Profiling and 3D Imaging. *Biosens. Bioelectron.* **2016,** *82*, 64-70.

57. Yang, L.; Guo, T.; Zhang, X.; Cao, S.; Ding, X., Toxic Chemical Compound Detection by Terahertz Spectroscopy: A Review. *Rev. Anal. Chem.* **2018,** *37*, 20170021.

 doi:10.20944/preprints202305.0200.v1